VOL. 11, NO. 7, APRIL 2016 ISSN 1819-6608
ARPN Journal of Engineering and Applied Sciences

www.arpnjournals.com

ROBUST AND EFFICIENT DIAGNOSIS OF CERVICAL CANCER IN PAP SMEAR IMAGES USING TEXTURES FEATURES WITH RBF AND KERNEL SVM CLASSIFICATION

S. Athinarayanan[1] and M. V. Srinath[2]
[1]Manonmaniam Sundaranar University, Abhisekapatti,Tirunelveli, Tamilnadu, India
[2]Department of MCA, STET Women's College, Sundarakkottai, Mannargudi. Trichy, Tamilnadu, India
E-Mail: aathithee@gmail.com

ABSTRACT

Classification of medical imagery is a difficult and challenging process due to the intricacy of the images and lack of models of the anatomy that totally captures the probable distortions in each structure. Cervical cancer is one of the major causes of death among other types of the cancers in women worldwide. Proper and timely diagnosis can prevent the life to some level. Consequently we have proposed an automated trustworthy system for the diagnosis of the cervical cancer using texture features and machine learning algorithm in Pap smear images , it is very beneficial to prevent cancer, also increases the reliability of the diagnosis. Proposed system is a multi-stage system for cell nucleus extraction and cancer diagnosis. First, noise removal is performed in the preprocessing step on the Pap smear images. Texture features are extracted from these noise free Pap smear images. Next phase of the proposed system is classification that is based on these extracted features, RBF and kernel based SVM classification is used. More than 94% accuracy is achieved by the classification phase, proved that the proposed algorithm accuracy is good at detecting the cancer in the Pap smear images.

Keywords: cervical cancer, feature extraction, classification.

1. INTRODUCTION

Cervical cancer is one of the decisive reasons of cancer death in females worldwide. The Pap smear is the great active screening test used to perceive the cervical pre-cancerous and cancerous variations in a experimental of cervical cells based on the shape variations of the nuclei and cytoplasm [1-3]. Pap test has severely altered the prediction of women with cervical cancer as it has revealed its ability to detect 95% of the cancers of the vaginal neck. Cervical cancer can be prevented if it is perceived and treated early [4]. Pap smear test is a physical screening process used to identify cervical cancer or precancerous changes in a uterine cervix by grading cervical cells based on color, shape and texture properties of their nuclei and cytoplasms. A computer-assisted screening structure for Pap smear tests will be exact helpful to prevent cervical cancer if it increases the reliability of the diagnosis[5]. Papanicolaon (PAP) Smear Screening Test is the most common form of diagnosis for detecting cervical cancer in its early stages. Cervical cancer is a disease that occurs when cells in the cervix area instigate to produce out of controller and attack nearby tissues or feast throughout the body. Cancer or tumor can be divided into two groups i.e. benign and malignant. Benign, that does not attack and abolish the tissue in which it originates or spread to aloof sites in the body (non-cancerous tumor) while malignant, that attacks and abolishes the tissue in which it invents and can feast to other sites in the body via blood-stream and lymphatic system (cancerous tumor) [6-8].

Medical image processing system has lead to an increasing important and evolving role for image processing and computer-aided diagnosis (CAD) systems in numerous clinical applications. Cervical cancer is the second most common cancer affecting women worldwide and the leading cause of cancer mortality in developing countries. It can be cured in almost all patients, if detected early and treated adequately. An automated image analysis system of uterine cervical images analyzes and extracts diagnostic features in cervical images and can assist the physician with a suggested clinical diagnosis. Such a system could be integrated with a medical screening device to allow screening for cervical cancer by non-medical personnel [9-10].

Image segmentation is a serious component of image recognition and analysis system. It plays a significant role in biomedical imaging applications such as the inventory of tissue volumes diagnosis, localization of pathology analysis of anatomical structure, treatment planning, partial volume upgrading of practical imaging data, and computer integrated surgery [11-12]. Medical Image segmentation is to partition the image into a set of regions that are visually obvious and consistent with respect to some properties such as gray level, texture or color. On the other hand, feature extraction is one of the most important methods for capturing visual content of an image. To facilitate decision making such as pattern classification, feature extraction is used as the process to represent the raw image in its reduced form. This approach combines the intensity, texture, shape based features and classifies the tumor as white matter, gray matter, CSF, abnormal and normal area. The various methods such as multi texton histogram (MTH), principal component analysis (PCA) Texton co-occurrence matrix and linear discriminant analysis (LDA) are used for reducing the

number of features [13]. The MTH is a feature extractor and a descriptor to retrieve the content image which integrates the advantages of representing the attribute of the co-occurrence matrix using histograms [14]. This descriptor analyzes the spatial correlation between neighboring color and edge orientation based on four special texton types [15].

The feature extraction plays an important role in cervical cancer classification process, whose effectiveness depends upon the method adopted for extracting features from given images. The visual content descriptors are either global or local. A global descriptor represents the visual features of the whole image; whereas a local descriptor represents the visual features of regions or objects to describe the image. These are arranged as multidimensional feature vectors and construct the feature database. For similarity distance measurement many methods have been developed like Euclidean distance (L2), L1 distance etc. Selection of feature descriptors and similarity distance measures affect performances of an Cervical cancer classification system significantly [16]. In this research article, we have developed a cervical cancer detection system that is able to detect and categorized cervical cells into normal and cancerous cells based on texture features and machine learning method. The rest of the paper is organized as follows: Our proposed technique is presented in section 2. The detailed experimental results and discussions are given in section 3, while the conclusion is summarized in section 4.

2. PROPOSED CERVICAL CANCER CLASSIFICATION SYSTEM

Classification of medical imagery is a knotty and challenging process due to the intricacy of the images and lack of models of the anatomy that completely captures the possible deformations in each structure. Cervical cancer is the supreme common malignancy in women in the emerging countries. Cervical cancer grows over a protracted period covering two to three decades. Cervical cancer is the most common form of cancer in women under 35 years of age and the second most commonly occurring cancer in women of all ages, worldwide [17]. In our proposed, cervical cancer classification systems consists of preprocessing, segmentation, feature extraction and feature classification. In feature extraction, multiple features are used to determine the relevance of normal and abnormal images. In this scenario, it is essential to minimize all the features distances that are determined between the cancer image and the non cancerous images. To perform the classification stage efficiently, an effective classification algorithm is required. In this research work, we exploit the proposed hybrid algorithm in the classification stage to ensure the classification performance. Our proposed method consists of three phases namely, Cervical Cell Nucleus Detection, feature extraction and classification. In this paper, Cervical Cell Nucleus Detection is done by using pre-processing and segmentation process. In pre-processing, anisotropic filter is applied to remove the noise and enhance the image for the cell Nucleus detection process.

2.1. Cervical cell nucleus detection

It is the crucial stage in the entire process. Pre-processing and segmentation process are the steps to the tumor region identification stage. Preprocessing on the input image is extremely essential, so that the image gets altered to be related to the further processing. In this paper, experimental images cannot be given directly the segmentation process. The input image is passed through an anisotropic filter which diminishes the noise and enhances the image quality. Anisotropic filter is used for reducing image noise without removing significant parts of the image content, particularly the edges, lines or other details that are important for the interpretation of the image [18]. The proposed cervical cell nucleus detection process consists of three stages such as

a) Image binarization using thresholding.
b) Sharpening the region using morphological operations.
c) Nucleus region identification

2.1.1 Original image is convert into a binary image by thresholding

Initially, the input image is transformed into a binary image. An image of up to 256 gray levels is translated to a black and white image using the threshold value. The gray level value of every pixel in the improved image is considered at this stage. All the pixels with values above the threshold are set as white and the remaining pixels are set as black in the image during the binarization process. In this paper, the threshold value is selected based on the contrast of the image as given in equation (1).

$$\text{Binarized Image, } B_{Binary}(k,y) = \begin{cases} 0, & if\ B_{grey}(k,y) =< Threshold \\ 1, & Otherwise \end{cases} \quad (1)$$

2.1.2 Sharpening the region using Morphological operation

After transforming into binary images, the morphological process is applied for sharpening the regions and filling the gaps. The main processes of the morphological operations are opening, closing, erosion and dilation. In this paper, erosion operation is applied for removing the hurdle, noise and enhances the image.

Erosion: In the erosion operation on an image F having labels 0 and 1 with structuring element Y, the value of pixel i in F is changed from 1 to 0, if the result of convolving Y with F, centered at i, is below some predefined value. We have set this value to be the area of Y, which is principally the number of pixels that are 1 in the structuring element itself. The structuring element,

also known as the erosion kernel, finds out the details of how particular erosion thins boundaries as given in equation (2).

$$IE = imerode(F, Y) \quad (2)$$

2.1.3 Nucleus area identification

After the morphological operation, the Nucleus regions are identified via a regionprops algorithm. The regions of the Nucleus are marked out based on their area properties. The regionprops algorithm measures the properties of image regions. Using the actual number of pixels in the region, the Nucleus region's area is segmented. This value is slightly different from the value returned by *bwarea,* which weights diverse patterns of pixels in a different way. The regionprops calculates the area by measuring the distance between each neighboring pair of pixels around the border of the region. After the segmentation process is completed, we get the segmented nucleus from its surrounding cytoplasm. But the results were somewhat light portioning of the nucleus. For this reason, authors have gone for the enhancement process to enhance or increase the contrast of the nucleus.

2.2 Feature extraction process

The process of extracting the features of the high contrast image sequence in a temporal frame with gray scale reference information for text block detection in both horizontal and vertical edge scanning of adjacent text block in a multi-resolution fashion are considered as feature extraction. It extracts information grounded on maximum gradient difference. The purpose of feature extraction is to reduce the original data set by measuring certain properties, or features, that distinguish one input pattern from another pattern. The extracted feature is expected to provide the characteristics of the input type to the classifier by considering the description of the relevant properties of the image into a feature space. The proposed method feature extraction process consists of five steps such as

- Computation of Feature Vector F(V1) using LoG
- Computation of Feature Vector F(V2) using GLCM
- Computation of Feature Vector F(V3) using DGTF
- Computation of Feature Vector F(V4 using RICGF
- Concatenation of four feature vector

2.2.1 Laplacian of Gaussian (LoG)

LoG filters at Gaussian widths of 0.25, 0.50, 1, and 2 are considered. These values are convoluted with the input image. Sixteen features are retrieved by calculating mean, standard deviation, skewness, autocorrelation, busyness, coarseness and kurtosis for the LoG filter output in the SROI region.

Mean: The mean (m) is defined as the sum of the intensity values of pixels divided by the number of pixels in the SROI of an image.

Standard deviation: It shows how much variation or exists from the expected value i.e., the mean. The data points tend to be very close to the mean results low standard deviation and the data points are spread out over a large range of values results high standard deviation.

Skewness: It is a measure of the asymmetry of the data around the sample mean. If the value is negative, the data are spread out more to the left of meaner than to the right. If the value is positive, the data are spread out more to the right. The sickness of the normal distribution (or any perfectly symmetric distribution) is zero. The skewness of a distribution is defined as given in equation (3).

$$Y=E(x-\mu)^3/\sigma^3 \quad (3)$$

Where μ is the mean of x, σ is the standard deviation of x, and $E(t)$ represents the expected value of the quantity t.

Autocorrelation: It is used to evaluate the quantity of promptness as well as the excellence of the texture present in the image, denoted as $f(\delta_i, \delta_j)$. For a n x m image is defined as follows and it was given in equation (4).

$$f(\delta_i, \delta_j) = \frac{1}{(n-\delta_i)(m-\delta_j)} \sum_{i=1}^{n-\delta_i} \sum_{j=0}^{m-\delta_j} I(i, j) I(i+\delta_i, j+\delta_j) \quad (4)$$

Here $1 \le \delta_i \le n$ and $1 \le \delta_j \le m$. δ_i and δ_j represent a shift on rows and columns, respectively.

Kurtosis: The forth central moment gives kurtosis. It gives the measure of closeness of an intensity distribution to the normal Gaussian shape as given in equation (5).

$$\text{Kurtosis} = \frac{1}{N} \frac{\sum_i \sum_j (I(i,j) - m)^4}{\text{std}^4} \quad (5)$$

Coarseness: The Coarseness is calculated based on the Shape. This value is not equal to zero then the segmented area has been affected by the tumor, otherwise the tumor does not affect the segmented area. It is the average number of maxima in the auto correlated images and original images. The coarseness (Cs) is calculated as follows and it was given in equation (6).

$$C_s = \frac{1}{0.5*(\frac{\sum_{i=1}^{n}\sum_{j=1}^{m} Max(i,j)}{n} + \frac{\sum_{i=1}^{n}\sum_{j=1}^{m} Max(i,j)}{m})} \quad (6)$$

Busyness: It is calculated based on connectivity, how much the pixels are connected is calculated that is above 5 then the segmented area has a tumor. The business' value is below 5 the segmented area does not have a tumor. The Busyness value is depending on Coarseness. If the value of Coarseness is high, the It is related to coarseness in the reverse order, that is when the business is low and it was given in equation (7).

$$B_s = 1 - C_s^{\frac{1}{\alpha}} \quad (7)$$

2.2.2 Computation of Feature Vector F(V2) using GLCM

Gray-level-based features: features based on the differences between the gray-level in the candidate pixel and a statistical value representative of its surroundings. It contains the second-order statistical information of neighboring pixels of an image. It is estimated of a joint probability density function (PDF) of gray level pairs in an image [19].

It can be expressed in the following equation (8)

$$P_\mu(i,j) \qquad (i,j = 0,1,2,...N-1) \quad (8)$$

Where i, j indicate the gray level of two pixels, N is the gray image dimensions, μ is the position relation of two pixels. Different values of μ decides the distance and direction of two pixels .Normally Distance (D) is 1,2 and Direction (θ) is 0^0, 45^0, 90^0, 135^0 are used for calculation [20].

Texture features can be extracted from gray level images using GLCM Matrix. In our proposed method, five texture features energy, and contrast, correlation, entropy and homogeneity are experiments. These features are extracted from the segmented MR images and analyzed using various directions and distances.

Energy expresses the repetition of pixel pairs of an image as given in equation (9).

$$k1 = \sum_{i=0}^{N-1}\sum_{j=0}^{k-1} p_\mu^2(i,j) \quad (9)$$

Local variations present in the image are measured by Contrast. If the contrast value is high means the image has large variations as given in equation (10).

$$k2 = \sum_{t=0}^{N-1} t^2 \left\{ \sum_{i=0}^{N-1}\sum_{j=0}^{N-1} P_\mu(i,j) \right\} \quad (10)$$

Correlation is a measure linear dependency of gray level values in co-occurrence matrices. It is a two dimensional frequency histogram in which individual pixel pairs are assigned to each other on the basis of a specific, predefined displacement vector as given in equation (11).

$$k3 = \sum_{i=0}^{k-1}\sum_{j=0}^{k-1} \frac{(i,j)\,p(i,j) - \mu_1\mu_2}{\sigma_1^2\sigma_2^2} \quad (11)$$

Where $\mu_1, \mu_2, \sigma_1, \sigma_2$ are mean and standard deviation values accumulated in the x and y directions respectively.

Entropy is a measure of non-uniformity in the image based on the probability of Co- occurrence values; it also indicates the complexity of the image as given in equation (12).

$$k4 = -\sum_{i=0}^{k-1}\sum_{j=0}^{k-1} p_\mu(i,j)\log(p_\mu(i,j)) \quad (12)$$

Homogeneity is inversely proportional to contrast at constant energy, whereas it is inversely proportional to energy as given in equation (13).

$$k5 = \sum_{i=0}^{k-1}\sum_{j=0}^{k-1} \frac{p_\mu(i,j)}{1+(i-j)^2}, i \neq j \quad (13)$$

2.2.3 Directional Gabor Texture Features (DGTF)

Directional Gabor's are used as they measure the heterogeneity in the SROI. Gabor filter is a Gaussian kernel function modulated by a sinusoidal plane wave. There-fore, it gives directional texture features at a specified Gaussian scale. Gabor kernel is defined as given in equation (14).

$$g(x,y,\lambda,\theta,\psi,\sigma,\gamma) = \exp\left(-\frac{x'^2+\gamma^2y'^2}{2\sigma^2}\right) \times \cos\left(2\pi\frac{x'}{\lambda}+\psi\right)$$

$$\text{where } x' = x\cos\theta + y\sin\theta,\ y' = -x\sin\theta + y\cos\theta' \quad (14)$$

In this equation, λ represents the wavelength of the sinusoidal factor, θ represents the orientation of the normal to the parallel stripes of a Gabor function, ψ is the phase offset, σ is the width of the Gaussian, and γ is the spatial aspect ratio, and specifies the ellipticity of the support of the Gabor function [21].

2.2.4 Rotation Invariant Circular Gabor Features (RICGF):

Gabor filter is a Gaussian kernel function modulated by a radially sinusoidal surface wave; therefore, it gives rotational invariant texture features which are given by eqn(15):

$$g(x,y,\lambda,\theta,\psi,\sigma) = \exp\left(-\frac{D(x,y)^2}{2\sigma^2}\right).\cos\left(2\pi\frac{D(x,y)}{\lambda}+\psi\right)$$
$$\text{where } D(x,y) = \sqrt{(x-\bar{x})^2+(y-\bar{y})^2} \quad (15)$$

Where, λ represents the wavelength of the sinusoidal factor, θ represents the orientation of the normal to the parallel stripes of a Gabor function, ψ is the phase offset, σ is the width of the Gaussian, and γ is the spatial aspect ratio, and specifies the ellipticity of the support of the Gabor function. The intensity and texture features summary is given in Table-1.

Table-1. Summary of intensity and texture features.

Feature category	Features	Number of features
LoG	Four statistical parameters for the LoG filter output in the SROI region are retrieved at σ = 0.25, 0.50, 1, and 2 thereby contributing 16 features in the feature pool. These parameters are: (1) mean intensity, (2) standard deviation, (3) Skewness, (4) Kurtosis	16 features
GLCM	Following GLCM features at 0°, 45°, 90°, and 135° are calculated: (1) contrast, (2) homogeneity, (3) correlation, (4) Energy	4*4 =16 features
DGTF	DGTFs are calculated at λ for 2√2, 4, 4√2, 8, 8√2) and θ for 0°, 22.5°, 45°, 67.5°, and 90° are varied. Four statistical parameters are calculated for each filter output in the marked SROI and are taken as 100 features in the feature bank. These parameters are: (1) mean intensity, (2) standard deviation, (3) Skewness, (4) Kurtosis	25* 4=100 features
RICGFs	RICGFs are calculated at λ =2√2, 4, 4√2, 8, 8√2) and two values of ψ, i.e., 0° and 90° four statistical parameters for each filter output in the marked SROI and are taken as 40 features in the feature bank. These features are: (1) mean intensity, (2) standard deviation, (3) Skewness, (4) Kurtosis	10* 4=40 features

2.3 Hybrid Kernel-SVM classifier

The diagnostic models, hybrid kernel based SVM has been developed for improving the classification process. The extracted textures features are used for the separation of two classes such as cancer and non-cancerous. Since the texture feature follows the non-linearity, non-linear SVM is needed to do the separation of hyperplane. To do non-linear task, kernel functions are introduced in SVM classification. Multiple kernels are combined to develop a new hybrid kernel that will improve the classification task of separating the training data. By introducing the hybrid kernel, SVMs gain flexibility in the choice of the form of the threshold, which need not be linear and even not to have the same functional form for all data, since its function is non-parametric and operates locally.

In most of the cases, an object is assigned to one of the several categories based on some of its characteristics in the real life situation. For instance, based on the outcome of several medical tests, it is mandatory to say whether the patient has a particular disease or not. In computer science such situations are explained as classification issue. There are two phases in the support vector machine namely, (1) Training phase and (2) Testing phase.

2.3.1. Training phase

The output from the improved multi-texton is given as input to the training phase. The input function gives the set of values which are non separable. All the possible separations of the pointset can be achieved by a hyperplane. For that, a set of data drawn from an unknown distribution, $((x_1, y_1),...,(x_1, y_l), x_i) \in R^n$, $y_i \in \{-1,1\}$ and also a set of decision functions, or hypothesis space $f_\lambda : \lambda \in \wedge$ are given, where Λ (an index set) is a set of abstract parameters, not necessarily vectors. $f_\lambda : R^n \to \{-1,+1\}$ is also called a hypothesis.

The set of functions f_λ could be a set of Radial Basis Functions or a multi-layer neural network. All the

possible separations of the point set can be achieved by a hyperplane. In the Lagrange optimization formulation we can find the optimal separating hyperplane normal vector,

A kernel is any function $K: R^n \times R^n \to R$. This corresponds to a dot product for some feature mapping as given in eqn(16)

$$K(X_1, X_2) = \phi(X_1).\phi(X_2) \text{ For some } \phi \quad (16)$$

The kernel function can directly compute the dot product in the higher dimensional space.

Introduce kernel- based Lagrange multipliers $\alpha_i \geq 0 \forall_i$ as given in eqn(17).

$$L_p = \sum_{i=1}^{n} \alpha_i - \frac{1}{2} \sum_{i=1}^{n} \sum_{i=1}^{n} \alpha_i \alpha_j y_i y_j K(x_i . x_j) \quad (17)$$

Minimize L_p with respect to w, b and maximize with respect to α_i.

In a convex quadratic programming problem, the plane is a nonlinear combination of the training vectors as given in eqn(18)

$$w = \sum_{i=1}^{n} \alpha_i y_i K(x_i) \quad (18)$$

Thus, the hyperplane is separated into two clusters. The sample representation of this process is shown in Figure-1.

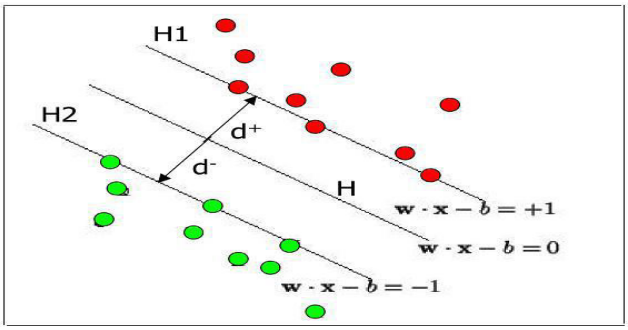

Figure-1. Sample representation of separating optimal hyper plane.

The point on the planes H_1 and H_2 is the Support Vectors. H_1 and H_2 are the planes:

d^+ = the shortest distance to the closest positive point

d^- = the shortest distance to the closest negative point

$d^+ + d^-$ Represents the margin of a separating hyper plane

2.3.2. Testing phase

The output from the improved multi-texon is given as an input cervical image to the testing phase and the output cervical image shows whether a tumor is present or not.

The class of an input data x is then determined in eqn (19)

$$class(x) = sign(\varphi(x).w - b) = sign\left(\sum y_i \lambda_i \varphi(x_i).\varphi(x) - b\right) \quad (19)$$

We have analyzed the kernel equation from the existing work [22] and used them in the proposed work namely, RBF and quadratic function.

Radial basis function: The support vector will be the centre of the RBF and σ will determine the area of influence. This support vector has the data space in eqn(20).

$$K(x_i, x_j) = \exp\left(-\frac{\left\|x_i - x_j\right\|^2}{2\sigma^2}\right) \quad (20)$$

Quadratic kernel function: Polynomial kernels are of the form $K(\vec{x}, \vec{z}) = (1 + \vec{x}^T \vec{z})^d$.

Where $d = 1$, a linear kernel and $d = 2$, a quadratic kernel are commonly used.

Let $k_1(RBF) and\ k_2(Quadratic)$ be kernels over $\Xi \times \Xi, \Xi \subseteq R^p$, and k_3 be a kernel over $R^p \times R^p$. Let function $\varphi: \Xi \to R^p$. The four kernel based formulations are represented by in eqn. (21and 22).

- $k(x, y) = k_1(x, y) + k_2(x, y)$ is a kernel (21)
- $k(x, y) = k_1(x, y) k_2(x, y)$ is a kernel (22)

Substitute the two equations (i) to (ii) in Lagrange multiplier equation (5) and get the proposed hybrid kernel. It is exposed in Equation (23).

$$L_p = \sum_{i=1}^{n} \alpha_i - \frac{1}{2} \sum_{i=1}^{n} \sum_{i=1}^{n} \alpha_i \alpha_j y_i y_j (k_1(x_i . x_j) + k_2(x_i x_j))$$

$$L_p = \sum_{i=1}^{n} \alpha_i - \frac{1}{2} \sum_{i=1}^{n} \sum_{i=1}^{n} \alpha_i \alpha_j y_i y_j k_1(x_i . x_j) k_2(x_i x_j) \quad (23)$$

Substitute the four theorems in Quadratic function equation (23) and get the given equation (24),

$$w = \sum_{i=1}^{n} \alpha_i y_i (K_1(x_i) + k_2(y_i))$$

$$w = \sum_{i=1}^{n} \alpha_i y_i \alpha K_1(x_i) k_2(y_i) \quad (24)$$

3. EXPERIMENTAL RESULTS AND COMPARATIVE ANALYSIS

3.1 Experimental image data set

The experimental Pap smear images are acquired through a powerful micro scope by the skilled cyto-technicians. All images were captured with a resolution of 0.201 μm/pixel from the open bench mark database of cervical cancer, Herlev University Hospital, Denmark [25-26]. The images were prepared and analyzed by the staff at the hospital using a commercial software package CHAMP2 for segmenting the images. Each image was examined and diagnosed by pathologists of that hospital before being used as reference for this study.

3.2 Experimental results

In this Experimental Result Section as per the three process of this paper which was referred in our previous section (2.1.1 -2.1.3), collected images could be processed. The Result was given in following Table-2.

Table-2. Experimental results.

S. No.	Input image (RGB image)	Gray image	Anisotropic filter image	Final nucleus detected image
1	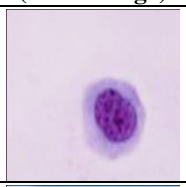	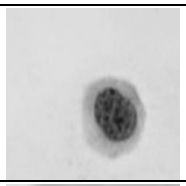	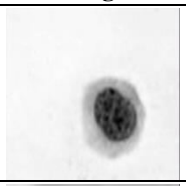	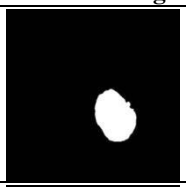
2				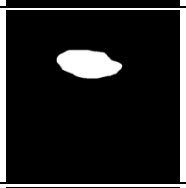
3	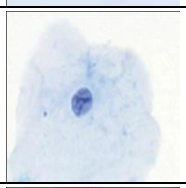	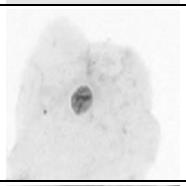	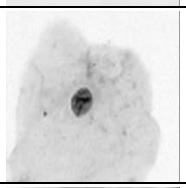	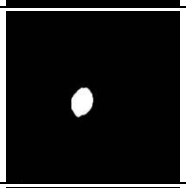
4	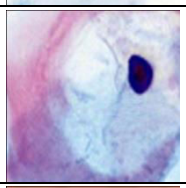	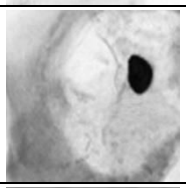	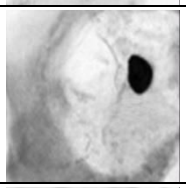	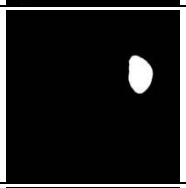
5		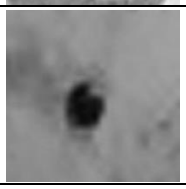	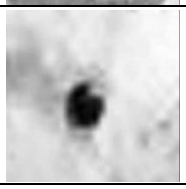	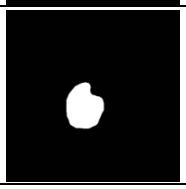

3.3 Performance evaluation of proposed system

Classifier performance evaluation of this work is conducted with widely used statistical measures, sensitivity, specificity, accuracy and error rate [23]. True Positive (TP) is defined as the number of correctly identified positive pixels; True Negative (TN) is defined

as correctly identified negative pixels. For example, in a diagnostic test, evaluation focusing on the presence of abnormal tissues, tumor samples is considered in the positive category and normal tissues will be in the negative category. False Positive (FP) represents the count of normal tissues incorrectly identified as a tumor, and False Negative (FN) gives the count of abnormal samples incorrectly identified as normal tissues. Higher values of sensitivity, the proportion of correctly classified positives, indicate better performance of the method in predicting positives. Specificity measures how well the system can predict the negatives. Accuracy measures the overall correctness of the classifier in predicting both positives and negatives, and overall error rate is calculated as per the following eqn (25-28).

$$Sensitivity = TP/(TP + FN) \quad (25)$$

$$Specificity = TN/(TN + FP) \quad (26)$$

$$Accuracy = (TN + TP)/(TN + TP + FN + FP) \quad (27)$$

$$Error\ rate = 1 - Accuracy \quad (28)$$

3.4. Comparative analysis

We have compared our proposed cervical cancer classification system, against the neural network techniques. The neural networks, we have utilized for comparative analysis are Feed Forward Neural Network (FFNN) and Radial Basis Function (RBF) neural network. The performance analysis has been made by plotting the graphs of evaluation metrics such as sensitivity, specificity and the accuracy are shown in Table-3.

Table-3. Experimental results of existing and proposed method.

Evaluation metrics		Texture features with HKSVM (Proposed)	Texture features with RBF	Texture features with FFNN
Input Cervical Cell image data set	TP	38	37	35
	TN	9	8	8
	FP	1	2	2
	FN	2	3	5
	Sensitivity	95	92.5	87.5
	Specificity	90	80	80
	Accuracy	94	90	86
Total error (%)		6	10	14

By analyzing the plotted graph; the performance of the proposed technique has significantly improved the tumor detection compared with Feed Forward Neural Network (FFNN) and Radial Basis Function (RBF) neural network classifier. The evaluation graphs of the sensitivity, specificity and the accuracy graph are shown in Figure-3. Based on the experimental results our proposed method produces better results compared to other neural network based classifiers. The Cervical cancer classification error bar is also given in Figure-4.

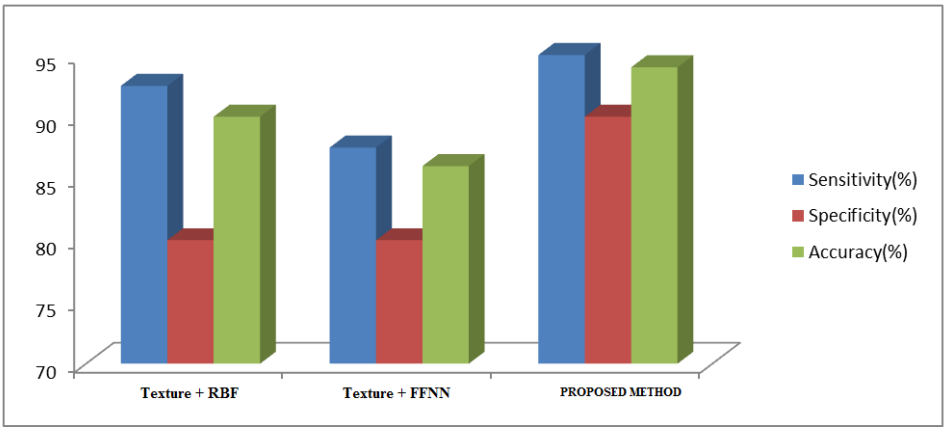

Figure-3. Comparison result analyses of Texture features with HKSVM, RBF and FFNN.

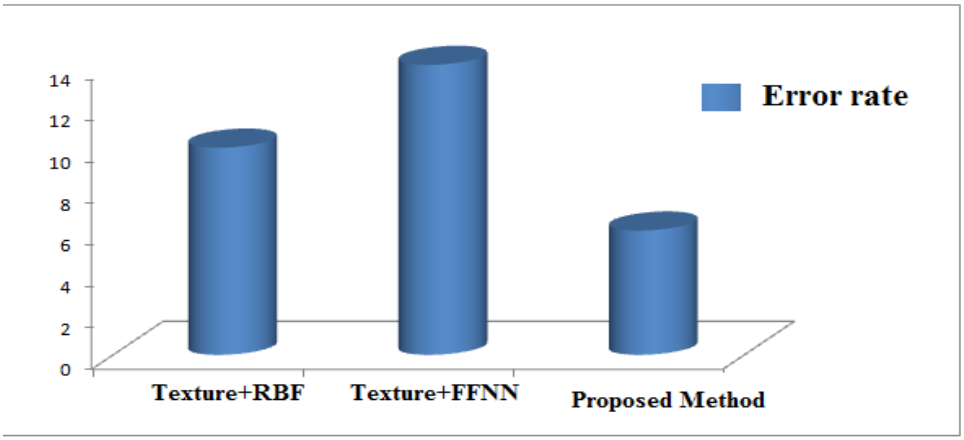

Figure-4. Comparison error bar of the proposed Texture features with various classifiers.

3.5 Comparative analysis using the K-fold cross-validation method

This section presents the performance analysis of the proposed system using K-fold cross-validation method [24]. According to this, the original data set of 100 images is divided into k subsets (k=10) of data and for every validation, a single subset is used as the testing data and the remaining subsets are utilized as training data. This procedure is repeated until all the subsets of data utilized as testing data. Here, we have chosen k=10 so that, the input data are divided into '10' sub-samples to extensively analyze the proposed system. The obtained experimental results of sensitivity of proposed method and existing methods using k-fold cross validation method are shown in Figure-5, it can be observed that the sensitivity of existing methods (Textures+SVM) is 0.81 for data set 1, but in the same data set the sensitivity of the proposed method is 0.93. Based on the experimental results, the sensitivity value of proposed method results is better compared to the existing methods.

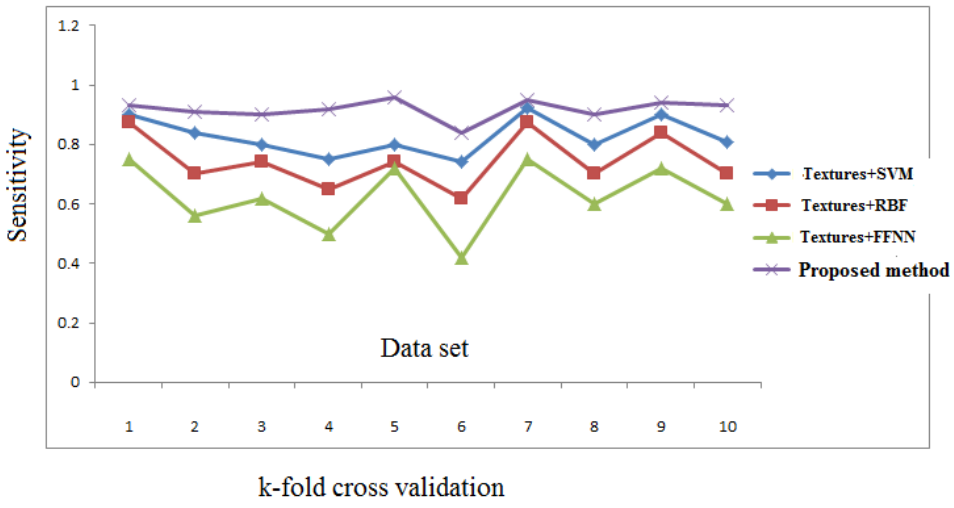

Figure-5. Comparison results of sensitivity of proposed and existing methods.

The obtained experimental results of specificity and accuracy of proposed and existing methods using k-fold cross validation method are shown in Figure-6 and Figure-7 respectively. In Figure-6, the specificity of existing methods (Textures+SVM]) is 0.82 for data set 1, but in the same data set the specificity of the proposed method is 0.92. Based on the observation, the specificity and accuracy value of proposed method results is better compared to the existing methods.

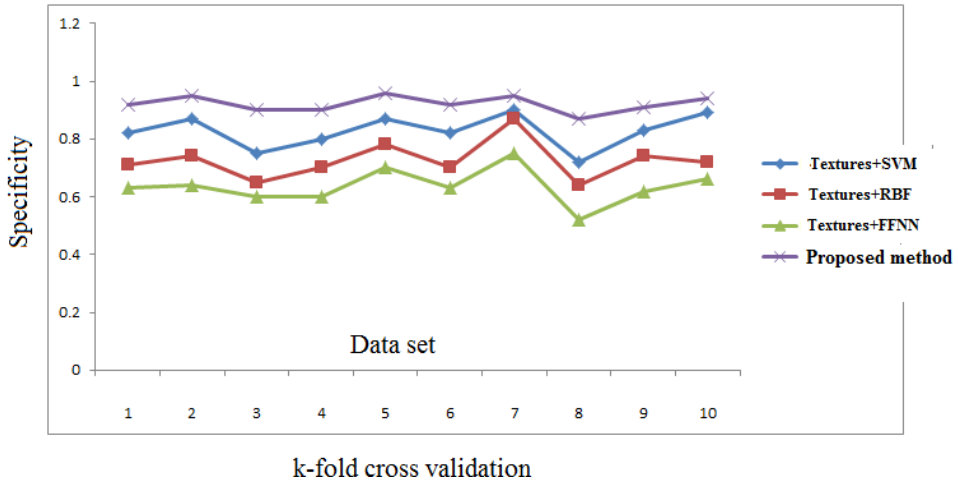

Figure-6. Comparison results of specificity of proposed and existing methods.

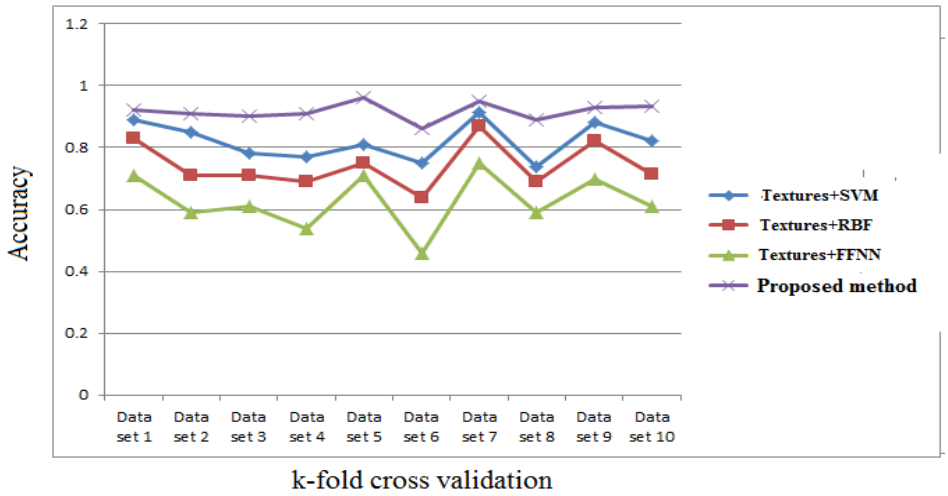

Figure-7. Comparison results of accuracy of proposed and existing methods.

4. CONCLUSIONS

In this paper, we have developed an automated cervical cancer diagnostic system with normal and abnormal classes. The medical decision making system was designed with the Texture features and kernel based Support Vector Machine. The proposed approach comprises feature extraction and classification. The benefit of the system is to assist the physician to make the final decision without hesitation. According to the experimental results, the proposed method is efficient for the classification of image into normal and abnormal. For comparative analysis, our proposed approach is compared with other neural networks RBF and FFNN. The accuracy level (94%) for our proposed method proved that the proposed algorithm graph is good at detecting the cancer in the experimental images.

REFERENCES

[1] Eko supriyanto, Nur azureen M. Pista, lukman hakim ismail, bustanur rosidi, tati latifah mengko. 2011. Automatic Detection System of Cervical Cancer Cells Using Color Intensity Classification. ISBN: 978-1-61804-019-0. Recent Research in Computer Science.

[2] Kiviat N. 1996. Natural History of Cervical Neoplasia: Overview and Update. Am J. of Obstet Gynecol. 175? 1099-1104.

[3] Kurman. R.J, D. E. Henson, A. L. Herbst, K. L. Noller and M. H. Schiffman. 1994. Interim guidelines of management of abnormal cervical cytology. J. Amer. Med. Assoc. 271: 1866-1869.

[4] Marinakis Y., Marinaki M., Dounias G. 2008. Particle swarm optimization for Pap-smear diagnosis. Expert Systems with Applications. 35: 1645-1656.

[5] Nandita Pradhan and Sinha. 2010. Development of a Composite Feature Vector for the Detection of Pathological and Healthy Tissues in FLAIR MR Images of Brain. Journal of ICGST-BIME. 10(1): 1-11.

[6] Mustafa N., Mat-Isa N. A., Ngah U. K., Mashor M. Y. and Zamli K. Z. 2004. Linear Contrast Enhancement Processing on Preselected Cervical Cell of Pap Smear Images. Technical Journal School of Electrical and Electronic Engineering, USM (ISSN: 1594-6153). 10. 30-34.

[7] Khotanlou H, Olivier Colliot, Jamal Atif, Isabelle Bloch. 2009. 3D brain tumor segmentation in MRI using fuzzy classification, symmetry analysis and spatially constrained deformable models. Fuzzy Sets and Systems. 160(10): 1457-1473.

[8] R. Mishra. 2010. MRI based brain tumor detection using wavelet packet feature and artificial neural networks. Proceedings of the International Conference and Workshop on Emerging Trends in Technology.

[9] Shan Shen, William Sandham, Malcolm Granat and Annette Sterr. 2005. MRI Fuzzy Segmentation of Brain Tissue Using Neighborhood Attraction with Neural-Network Optimization. IEEE Transactions on Information Technology in Biomedicine. 9(3).

[10] Jzau-Sheng Lin, Kuo-Sheng Cheng and Chi-Wu Mao. 1996. Segmentation of Multispectral Magnetic Resonance Image Using Penalized Fuzzy Competitive Learning Network. Computers and Biomedical Research. 29: 314-326.

[11] Detection of Nuclei Clusters from Cervical Cancer Microscopic Imagery Using C4.5. Yu Peng1, Mira Park1, Min Xu1, Suhuai Luo1, Jesse S.Jin1, Yue Cui1, W. S. Felix Wong. 2010. Proceedings of 2nd International Conference on Computer Engineering and Technology [Vol. 3].

[12] 2008. Edge Enhancement Nucleus and Cytoplast Contour Detector of Cervical Smear Images: Shys-Fan Yang-Mao, Yung-Kuan Chan, and Yen-Ping Chu. IEEE Transactions on System Cybernatics. 38(2).

[13] Mustafa N., Mat-Isa N.A., Ngah U.K, Mashor M.Y and Zamli K.Z. 2014. Linear Contrast enhancement processing on preselected cervical cell of pap smear images. Technical Journal School of electrical and electronic engineering. USm (ISSN: 1594-6153). 10-30-34.

[14] Jayachandran A and R.Dhanasekaran. 2013. Brain Tumor Detection using Fuzzy Support Vector Machine Classification based on a Texton Co-occurrence Matrix. Journal of imaging Science and Technology. 57(1): 10507-1-10507-7(7).

[15] Julesz B. Textons, the elements of texture perception and their interactions. Nature. 290: 91-97. 1981

[16] Susanta Mukhopadhyay and Bhabatosh Chanda. 2003. Multiscale Morphological Segmentation of Gray Scale Image. IEEE Transactions on Image Processing. 12(5).

[17] Mustafa N., Mat-Isa N. A., Ngah U. K., Mashor M. Y. and Zamli K. Z. 2004. Linear Contrast Enhancement Processing on Preselected Cervical Cell of Pap smear Images. Technical Journal School of Electrical and Electronic Engineering, USM (ISSN: 1594-6153). 10. 30-34.

[18] Demirkaya O. 2002. Anisotropic diffusion filtering of PET attenuation data to improve emission images. Phys MED Biol. 47(20): N271-8.2002.

[19] Cobzas D, Birkbeck N, Schmidt M, Jagersand M, Murtha A. 2007. 3D variational brain tumor segmentation using a high dimensional feature set. In: Presented at computer vision, 2007. IEEE 11th International Conference on ICCV.

[20] Daugman JG. 1988. Complete discrete 2-D Gabor transforms by neural networks for image analysis and compression. IEEE Trans Acoustics Speech Signal Process. 36(7): 1169-79.

[21] Lee TS. 2006. Image representation using 2D Gabor wavelets. IEEE Trans Pattern Anal Math Intell. 18(10): 959-71.

[22] Long Chen, C. L. Philip Chen, Fellow, IEEE, and Mingzhu Lu. 2011. A Multiple-Kernel Fuzzy C-Means Algorithm for Image Segmentation. IEEE Transactions on Systems, Man, and Cybernetics-Part B: Cybernetics. 41(5): 1263- 1274.

[23] Wen Zhu, Nancy Zeng, Ning Wang. 2010. Sensitivity, Specificity, Accuracy, Associated Confidence Interval and ROC Analysis with Practical SAS Implementations. Proceedings of the SAS Conference, Baltimore, Maryland. p. 9.

[24] Ounpraseuth S, Lensing SY, Spencer HJ, Kodell RL. 2012. Estimating misclassification error: a closer look at cross-validation based methods. BMC Res Notes. 5(28): 656.

[25] E. Martin, Papsmear classification [M.S. thesis], Oersted DTU, Automation, Tech. Univ. Denmark, Copenhagen, Denmark, 2003.

[26] MDE Lab, http://labs.fme.aegean.gr/decision/downloads.